ChemPubSoc Europe

DOI: 10.1002/open.201600120

Open Access ChemistryOPEN Full Papers

Chiral Brønsted Acid-Catalyzed Enantioselective α-Amidoalkylation Reactions: A Joint Experimental and Predictive Study

Eider Aranzamendi,[a] Sonia Arrasate,[a] Nuria Sotomayor,[a] Humberto González-Díaz,*[a, b] and Esther Lete*[a]

Enamides with a free NH group have been evaluated as nucleophiles in chiral Brønsted acid-catalyzed enantioselective α-amidoalkylation reactions of bicyclic hydroxylactams for the generation of quaternary stereocenters. A quantitative structure–reactivity relationship (QSRR) method has been developed to find a useful tool to rationalize the enantioselectivity in this and related processes and to orient the catalyst choice. This correlative perturbation theory (PT)-QSRR approach has been used to predict the effect of the structure of the substrate, nucleophile, and catalyst, as well as the experimental conditions, on the enantioselectivity. In this way, trends to improve the experimental results could be found without engaging in a long-term empirical investigation.

1. Introduction

The intermolecular α-amidoalkylation reaction is a very useful carbon–carbon bond-forming process in organic chemistry.[1] It has been widely applied to the stereocontrolled functionalization of nitrogen heterocycles, as the reaction of the cyclic *N*-acyliminium ion intermediates, generated in situ, is usually highly diastereoselective.[2] The possibility of using a broad variety of nucleophiles[3] confers upon the reaction a very wide scope, and it has been employed in natural product and pharmaceutical syntheses.[4] In recent years, the enantioselective α-amidoalkylation reaction using organocatalysis has emerged as a powerful method for the synthesis of enantio-enriched compounds possessing tertiary or quaternary stereogenic centers.[5] The most important developments in this area have focused on enantioselective Friedel–Crafts-type reactions.[6] In particular, a number of reports have addressed the application of chiral hydrogen-bond donors (ureas and thioureas)[7] and chiral Brønsted acids (CBAs) (BINOL-derived phosphoric acids)[8] to the asymmetric intermolecular α-amidoalkylation reaction[9] of π-nucleophiles, mainly electron-rich heteroaromatics such as indoles and pyrroles[10] with cyclic *N*-acyliminium ions. However, limitations remain on the applicability for tertiary *N*-acyliminium ions (i.e. ketone-derived iminium ions), which can lead to synthetically important derivatives with chiral quaternary carbon centers, presumably owing to the low reactivity of ketimines and the more difficult control of facial selectivity.[11] In this context, we have reported[12] the first example of an enantioselective α-amidoalkylation of indoles with bicyclic α-hydroxylactams for the generation of a quaternary stereocenter in the preparation of 12b-substituted isoindoloisoquinolines (*ee* up to 95%) by using BINOL-derived Brønsted acids. The α-amidoalkylation reaction occurs through the formation of a chiral phosphate/bicyclic quaternary *N*-acyliminium ion pair. There was experimental evidence to propose that hydrogen-bonding interactions of the phosphate-ion-paired intermediate to the indole N–H could potentially be involved. Hence, the BINOL-derived phosphoric acid would be acting as a bifunctional catalyst,[13] interacting also with the nucleophile. More recently, the same methodology has been applied by Li and coworkers[14] to the functionalization and preparation of isoindolo-β-carbolines, generally with high enantioselectivities (up to >99% *ee*). The potential of this type of hydroxylactam in stereochemical control has previously been demonstrated in transfer hydrogenation[15] and alkenylation[16] reactions. In the latter case, the presence of a hydroxyl group in the nucleophile, an *o*-hydroxystyrene, was crucial for the generation of a hydrogen bond with the chiral phosphoric acid catalyst. In a similar way, in the asymmetric organocatalytic aza-Friedel–Crafts reaction of ketimines with naphthols/phenols catalyzed by quinine-squaramide catalysts, the formation of a hydrogen bond between the phenolic OH and the tertiary amine moiety

[a] Dr. E. Aranzamendi, Dr. S. Arrasate, Prof. N. Sotomayor, Prof. H. González-Díaz, Prof. E. Lete
Departamento de Química Orgánica II, Facultad de Ciencia y Tecnología
Universidad del País Vasco/Euskal Herriko Unibertsitatea (UPV/EHU)
Apdo. 644, 48080 Bilbao (Spain)
E-mail: humberto.gonzalezdiaz@ehu.eus
esther.lete@ehu.eus

[b] Prof. H. González-Díaz
IKERBASQUE
Basque Foundation for Science
48080 Bilbao (Spain)

Supporting Information and the ORCID identification number(s) for the author(s) of this article can be found under http://dx.doi.org/10.1002/open.201600120.

of catalyst is proposed to explain the stereochemical outcome of the reaction.[17] On the other hand, a chiral phosphoric acid-catalyzed enantioselective α-alkylation of enamides with indolyl methanols[18] and 3-hydroxyoxindoles[19] has been reported, and its utility demonstrated in the total synthesis of (−)-folicanthine.

In this context, we decided to evaluate enamides **2** with a free N–H group in the enantioselective α-amidoalkylation reaction with bicyclic α-hydroxylactams **1** derived from phthalimides, using chiral phosphoric acids as Brønsted acid catalysts (Scheme 1). This would allow the enantioselective formation of

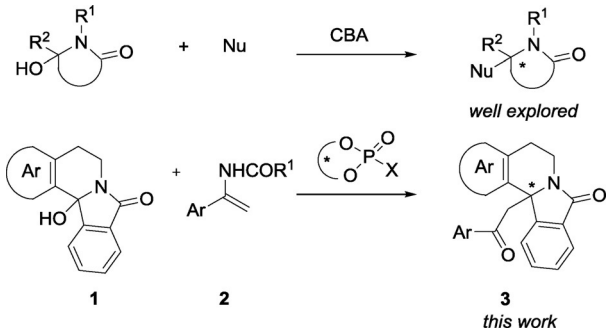

Scheme 1. Catalytic enantioselective intermolecular α-amidoalkylation reactions.

a quaternary stereocenter at the C-1 position of the tetrahydroisoquinoline unit of the isoindoloisoquinoline skeleton. It should be pointed out that tetrahydroisoquinoline is a privileged heterocyclic core present in many biologically active natural products and pharmaceutical drugs.[20] For example, C-1 indol-3-yl substituted 1,2,3,4-tetrahydroisoquinoline ISA-2011B (Figure 1) was found to have a potent inhibitory effect on proliferation in various types of aggressive cancer cell lines (for the treatment of advanced prostate cancer).[21] The isoindole motif is also a crucial structure in a number of molecules with pharmaceutical properties,[22] such as (*S*)-pazinaclone or

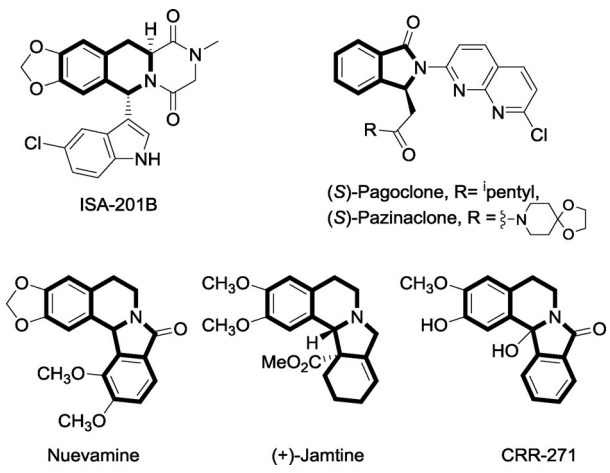

Figure 1. Selected bioactive compounds that contain isoindole and tetrahydroisoquinoline units.

(*S*)-pagoclone, and C(3)-substituted isoindolinones that are central nervous system (CNS) active drug candidates.[23] Therefore, the development of new synthetic methods for the asymmetric synthesis of these heterocycles continues to be an intensely investigated field.[24] Besides, alkaloids with the isoindolo[2,1-*a*]isoquinoline skeleton, such as hirsutine, jamtine, and nuevamine,[25] combine the structural features of both skeletons and also display a wide spectrum of biological activities. In fact, isoindoloisoquinolinone CRR-271 has been reported to inhibit PARP-1 activity and protect cells against oxidative DNA damage, which could be implemented in the treatment of inflammatory diseases.[26]

2. Results and Discussion

On the basis of our previous report, we initiated this study by evaluating the reaction of hydroxylactam **1a** with enamide **2a** to obtain enantio-enriched **3aa** (Table 1). Phosphoric acids **4a–e** and *N*-triflylphosphoramides **5a–h** were tested at room temperature in THF.[12] Significant differences in both reactivity and enantioselectivity were observed. Phosphoric acid **4a** was the most reactive, affording **3aa** in good yield (70%) after 24 h, but with no enantioselectivity (Table 1, entry 1).

On the contrary, no reaction was observed with **4b** after 72 h (Table 1, entry 2). The best enantioselectivity was observed when **4d** was used, although the yield was poor (Table 1, entry 4). *N*-Triflylphosphoramides are known to have an increased acidity, and may lead to the formation of tighter ion pairs.[27] Indeed, **5a–h** proved to be more reactive, affording significantly higher yields and reducing the reaction time to 5 h in most cases (Table 1, entries 6–13). Unfortunately, only low enantioselectivities were obtained. At lower temperatures, the reaction time was extended, with no significant improvement in enantioselectivity (Table 1, entry 9). It is important to note the different performances of catalysts **4d** and **5d**, which have the same substitution pattern on the aromatic backbones. Although **5d** was more reactive, an unexpected drop in the enantioselectivity (49 vs. 4%) was observed. Highly hindered (*R*)-VAPOL-derived phosphoric acid **6**[28] or multidentate disulfonimide **7**[29] afforded good reactivity, but low enantioselectivity (entries 15 and 16), whereas TADDOL-derived phosphoric acid **8**[30] was not reactive (entry 17).

A subsequent optimization of the reaction conditions was carried out by using catalyst **4d**, which had afforded the highest *ee* (49%). Both the reactivity and the enantioselectivity were improved when the reaction was performed at 40 °C (Table 2, entry 1). Besides, this enantioselectivity could be improved through a single crystallization to 84% *ee*. The use of an excess (3 equiv) of **2a** significantly lowered the yield and enantioselectivity (entry 2), probably owing to self-condensation of the enamide,[31] whereas the use of molecular sieves to remove the water formed in the reaction did not improve the results (entry 3). At higher temperature, the results were similar, but the reaction time was reduced (entry 4). The change of the solvent to dioxane afforded **3aa** with similar enantioselectivity, but lower yield (entry 5). The best yield was obtained when the reaction was performed in dichloromethane at reflux

Table 1. Evaluation of catalysts.

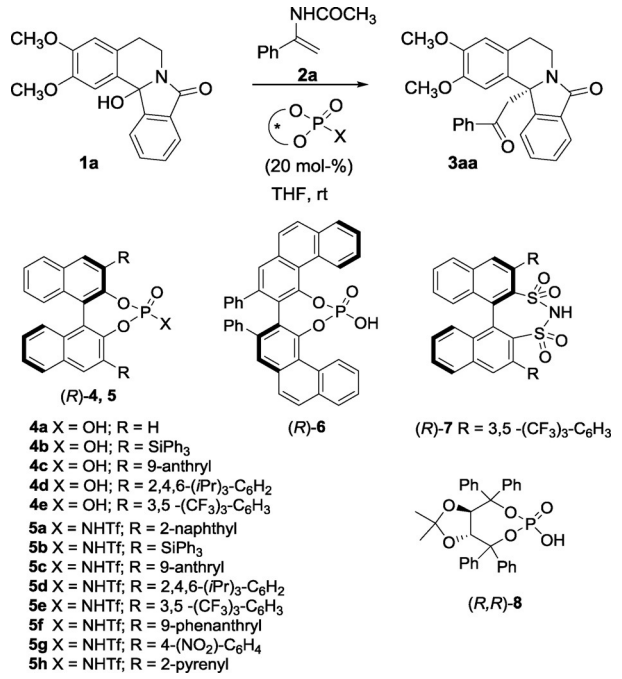

Entry	Catalyst	*t* [h]	Yield [%][a]	*ee* [%][b]
1	**4a**	24	70	0
2	**4b**	72	–[c]	–
3	**4c**	96	56	31
4	**4d**	72	15	49
5	**4e**	48	45	22
6[d]	**5a**	24	80	10
7	**5b**	5	55	5
8	**5c**	5	80	31
9[e]	**5c**	16	78	38
10	**5d**	5	84	4
11	**5e**	5	75	5
12	**5f**	5	83	28
13	**5g**	5	45	0
14	**5h**	5	83	18
15[d]	**6**	60	82	6
16	**7**	72	90	12
17[d]	**8**	96	10	2

[a] Yield of isolated product. [b] Determined by chiral stationary phase HPLC. [c] No reaction. [d] 40 °C. [e] −40 °C.

Table 2. Optimization of reaction conditions.

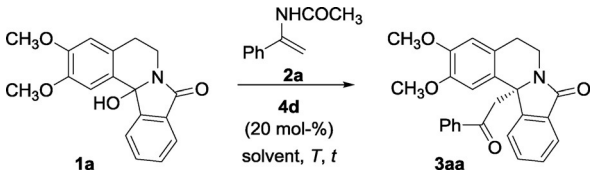

Entry	Solvent	*T* [°C]	*t* [h]	Yield [%][a]	*ee* [%][b]
1	THF	40	96	60	56 (84)
2[c]	THF	40	96	30	32
3[d]	THF	40	96	52	43
4	THF	reflux	60	50	45
5	dioxane	40	96	40	60 (80)
6	CH_2Cl_2	Rt	96	76	31
7[e]	CH_2Cl_2	40	48	95	40
8	DCE	40	72	76	31
9	toluene	40	96	51	60
10	toluene	reflux	60	65	42

[a] Yield of isolated product. [b] Determined by chiral stationary phase HPLC. [c] 3 equiv of **2a** were used. [d] Molecular sieves (4 Å) were added.

Table 3. Effect of the substitution on the enamide.

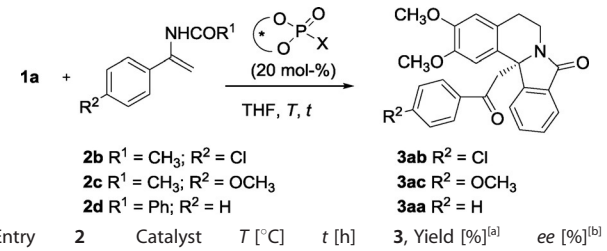

Entry	**2**	Catalyst	*T* [°C]	*t* [h]	**3**, Yield [%][a]	*ee* [%][b]
1	**2b**	**4d**	40	96	**3ab**, –[c]	–
2	**2c**	**4d**	40	96	**3ac**, 70	56
3	**2d**	**4d**	40	96	**3aa**, –[c]	–
4[d]	**2d**	**4d**	40	96	**3aa**, 50	24
5	**2d**	**5c**	rt	5	**3aa**, 60	31

[a] Yield of isolated product. [b] Determined by chiral stationary phase HPLC. [c] No reaction. [d] Toluene was used as solvent.

(95%, entry 7). Unfortunately, the enantioselectivity did not increase accordingly. In related chiral phosphoric acid-catalyzed reactions, it has been shown that the formation of ion pairs is favored in CH_2Cl_2 over THF, although it was found that the degree of ion-pair formation does not correlate with the enantioselectivity.[32] The use of toluene provided similar results to those obtained in THF (entry 9), and again further increase of the temperature was detrimental (entry 10). Next, the effect of the substitution pattern on the enamide was studied. Thus, enamides **2b–d** were prepared[33] and reacted with hydroxylactam **1a** by using phosphoric acid **4d** or triflamide **5c** as catalysts in THF (Table 3). The electronic nature of the aromatic ring had a strong influence on the reactivity, as no reaction was observed with **2b** (entry 1), whereas a good yield was obtained with electron-rich **2c**, although with no increase in the enantiomeric purity (entry 2). The effect of the acyl terminus of the enamide was also checked, but the corresponding benzamide **2d** did not improve the enantioselectivity when using **4d** or **5c** (Table 3, entries 4 and 5 vs. Table 2, entry 9 and Table 1, entry 8).

As shown, the enantioselectivity could be improved through a single crystallization. Thus, the absolute configuration was unambiguously assigned by single-crystal X-ray analysis of **3aa** as *R* (see the Supporting Information).[34]

The formation of the *R* isomer in the reaction of **1a** with enamides is in consonance with our previous results for the α-amidoalkylation of indoles.[12] Thus, the sense of induction would be explained by the formation of an *N*-acyliminium intermediate/chiral conjugate-base ion pair,[35] as depicted in Figure 2. Thus, the chiral ion pair would be generated by protonation of the hydroxylactam. According to previously reported models,[36] the acyliminium intermediate would be oriented avoiding the steric interactions with the catalyst **3** and **3**′-sub-

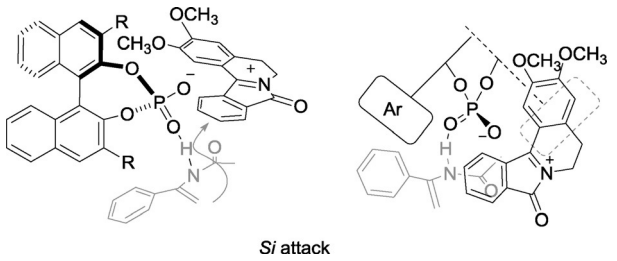

Figure 2. Proposed working model for the α-amidoalkylation reaction.

stituents (*R*). On the other hand, a hydrogen bond with the enamide N–H moiety could be proposed, which would orient the phenyl ring away from the catalyst, favoring the *Si* attack of the nucleophile.

We next studied the use of indole-derived hydroxylactam **1b** in the reaction with enamide **2a** (Scheme 2). The reaction of hydroxylactam **1b** under chiral phosphoric acid catalysis with different nucleophiles has been described previously.[14–16] We thought that the chiral phosphoric acid may act as a bifunctional catalyst, coordinating not only to the enamide but also to the indole NH.[37] Indeed, when hydroxylactam **1b** was treated with enamide **2a** and phosphoric acid **4d** in THF at room temperature, the reaction was much faster, leading to a good yield of β-carboline **3ba** in just 5 h. Unfortunately, the enantioselectivity was in the same range to that observed for **1a**. Similar results were obtained when a catalyst with the opposite configuration [(***S***)-**4d**] was used in dioxane.[38]

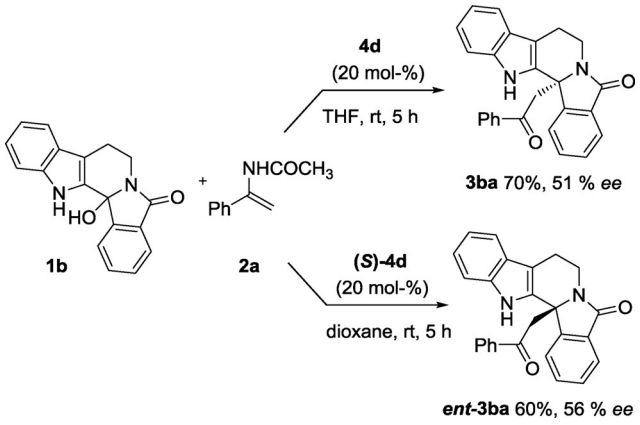

Scheme 2.

To check if the interaction of the enamide with the catalyst is really determinant, related reactions of hydroxylactams **1a** and **1b** were carried out using enol ethers **9a** and **9b** as nucleophiles (Table 4).

Enol ether **9a** was unreactive towards **1a** in THF and provided a very low conversion in dichloromethane (Table 4, entries 1 and 2). In contrast, **1b** reacted with **9a** (Table 4, entry 3), but the reaction was slower and less efficient than the reaction with the corresponding enamide **2a**, as depicted in Scheme 2, though with the same degree of enantioselectivity (51% *ee*). Changing the solvent did not improve the results. Finally,

Table 4. Reaction with enol ethers **9a** and **9b**.

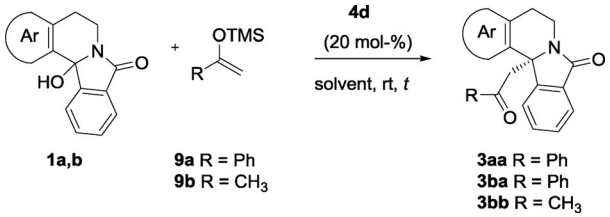

Entry	1	9	Solvent	*t* [h]	3, Yield [%][a]	*ee* [%][b]
1	**1a**	**9a**	THF	72	**3aa**, –[c]	–
2[d]	**1a**	**9a**	CH_2Cl_2	72	**3aa**, 10	−16
3	**1b**	**9a**	THF	48	**3ba**, 35	51
4[d]	**1b**	**9a**	CH_2Cl_2	48	**3ba**, 42	−14
5	**1b**	**9a**	toluene	48	**3ba**, 50	43
6	**1b**	**9b**	THF	48	**3bb**, –[c]	–
7	**1b**	**9b**	CH_2Cl_2	48	**3bb**, 20	56
8	**1b**	**9b**	toluene	48	**3bb**, 18	86

[a] Yield of isolated product. [b] Determined by chiral stationary phase HPLC. [c] No reaction. [d] ***(S)*-4d** was used as the catalyst.

when enol ether **9b** was used, **3bb** was obtained with good enantioselectivity in toluene (86% *ee*), though with a low conversion. These results show that, although coordination with the catalyst seems to be crucial for reactivity, there is not a direct effect on the enantioselectivity.

As noted above, the enantioselectivity is especially sensitive to the nature of the nucleophile and the catalyst, as well as the experimental conditions. As shown, the introduction of a chlorine atom into the aromatic ring of acetamide **2b** precluded the reaction, whereas the use of benzamide **2d** reduced the enantioselectivity as compared to the acetamides. Unfortunately, the optimal catalyst for **2a** led to poor enantioselectivities with the other enamides or enol ethers, and no obvious trends to improve the performance of these nucleophiles were qualitatively observed. The general catalytic cycle for this type of α-amidoalkylation reaction is now reasonably well established; however, the key catalyst features and experimental conditions responsible for enantioselection remain challenging. Thus, although there are detailed studies of the chiral phosphoric acid-catalyzed reduction of ketimines,[39] the origin of the stereochemical outcome in the carbon–carbon bond-forming reaction of ketimine has scarcely been investigated.[39b] In fact, it was not until very recently that the Friedel–Crafts reaction of 2-methoxyfuran with aliphatic ketimines was studied theoretically by using DFT calculations to assess the key factors governing the stereoselectivity. Thus, Terada and co-workers[40] analyzed the plausible transition states of the stereo-determining C–C bond-forming step, proposing that enantioselectivity stems from the formation of the hydrogen-bond network among the triad of components (catalyst, substrate, and nucleophile). Although computational chemistry has helped us to understand the mechanism of these α-amidoalkylation reactions, understanding how the different parameters affect its stereochemical outcome is still difficult to rationalize. This is one of the underlying challenges in the field of asymmetric catalysis: to design or choose the adequate cat-

alyst or experimental conditions for a given reaction type without engaging in a long-term, empirical investigation. Therefore, we sought to use chemoinformatic tools to predict the enantioselectivity of this type of intermolecular α-amidoalkylation reaction. We decided to use quantitative structure–reactivity relationship (QSRR) methods.[41] At this point, the pioneering work of Sigman and co-workers[42] should be pointed out, who demonstrated that a QSRR model between steric parameters of chiral ligand substituents and enantiomeric ratios of the products could be established. Since then, methodologies based on QSRR modeling have been applied to predict the enantioselectivity of different types of reactions, such as allylation[43] and propargylation[44] of carbonyl compounds, dehydrogenative Heck-type[45] reactions, asymmetric copper-catalyzed cyclopropanation of alkenes,[46] and the Henry reaction.[47] Recently, a data-intensive approach has also been reported for mechanistic elucidation applied to chiral anion catalysis in intramolecular dehydrogenative C–N coupling.[48] In this case, catalyst–substrate association involves weak, non-covalent interactions similar to those involved in the α-amidoalkylation reactions.

2.1. Predictive Study

We have previously developed a PT-QSPR approach, which combines perturbation theory (PT) and QSRR ideas, to correlate and predict different outputs (activity, property) in complex molecular systems (metabolic reactions),[49] nanoparticles,[50] and so forth. The method has also been extended to predict the enantioselectivity and/or yield of intramolecular carbolithiation[51] and Heck–Heck cascade reactions.[52] In some cases, the developed PT-QSRR models use trace operators, like spectral moments, or eigenvalues of chemical structure matrices, like bond adjacency matrix, as the inputs.[53,51] Now, we intend to use this correlative PT-QSRR approach to predict the effect of the structures of the substrate, nucleophile, and catalyst, as well as the experimental conditions, on the enantioselectivity of intermolecular α-amidoalkylation reactions. The model predicts the enantiomeric excess *ee*(%)nr of a new reaction (nr) by comparison to a reaction of a reference (rr) with known enantiomeric excess *ee*(%)rr that involves a set of molecules (mq), which play different roles (substrate, catalyst, etc.) similar to the new reaction (see the Supporting Information). Our goal is to find a useful tool to rationalize the enantioselectivity in this and related processes and to orient the catalyst choice. In this way, trends to improve the experimental results could be found.

To accomplish this, a large dataset of α-amidoalkylation reactions was compiled. This dataset included the above-described reactions and literature data for related reactions with different types of substrates (cyclic and bicyclic hydroxylactams), nucleophiles (enamides, indoles, etc.), and chiral catalysts (phosphoric acids, phosphoramides, etc.) under different experimental conditions.[12,15,18,19,54] The molecular descriptors *V*(mq) used to quantify the chemical structure of all the molecules involved in the reaction were calculated with the software DRAGON.[55] These molecular descriptors were the absolute eigenvalues of the matrix of topological distance weighted with atomic polarizabilities *V*(mq) = *AEigpq*. To find the QSRR model, a multivariate linear regression (MLR) analysis was performed with the software STATISTICA,[56] combining forward stepwise and standard procedures of variable selections (see the Supporting Information).

Then, we initiated the study with the training and validation of the new PT-QSRR model for the enantioselectivity of the reactions under study. We found a model useful to predict the efficiency of the new reaction $ee(\%)_{new}$, given the expected value of efficiency $ee(\%)_{expected} = <ee(\%)>_{new}$ for any new reaction in the solvent used and the values of the perturbation terms. The equation of this model is the correlation function shown in [Equation (1)]:

$$\begin{aligned} ee(\%)_{new} = {} & 0.558333 + 0.316901 \cdot g_{0new} \cdot \langle ee(\%)\rangle_{new} \\ & -0.000699 \cdot g_{0new} \cdot g_{4new} \\ & +0.132149 \cdot g_{0new} \cdot Y_{sub} \cdot \Delta V(\text{sub}) \\ & -0.001459 \cdot g_{0new} \cdot Y_{prod} \cdot \Delta V(\text{prod}) \\ & -0.011935 \cdot g_{0new} \cdot Y_{cat} \cdot \Delta V(\text{cat}) \\ & -0.136922 \cdot g_{0new} \cdot Y_{nuc} \cdot \Delta V(\text{nuc}) \\ & -0.000373 \cdot g_{0new} \cdot Y_{solv} \cdot \Delta V(\text{solv}) \end{aligned} \quad (1)$$

$$n = 38419\_R = 0.93\_F = 36394.0\_p < 0.005$$

All of the variables of the model (Table 5) are statistically significant, according to student test (see values of *t* and the *p*-level in Table 6). A notable feature of this model is its ability to predict a high number of perturbations in intermolecular α-amidoalkylation reactions ($n = 38\,419$) with high goodness-of-fit $R = 0.93$ (86.5% of variance of data explained). The model was validated with an external validation series of a large dataset of perturbations in intermolecular α-amidoalkylation reactions ($n = 12\,806$). Notably, the goodness-of-fit for the external validation series was also high $R = 0.93$ (Table 6). The chemical data associated with this PT-QSRR model, as well as the observed and predicted values of *ee*(%), are listed in the Supporting Information. The new PT-QSRR model reported here allows both the computational screening of a very large set of reac-

Table 5. Definition of all the terms used in the model.[a]

Factor	Switching function	Intensity coefficient
catalyst chirality	$\gamma 0 = g_{0new} = g_{0new}$	$g_{0new} = (R/S)$cat
additive	$\gamma 1 = g_{0new}\ (g_{1new}/g_{1ref})$	$g1 = (\text{TMSCl(eq)} + 1)$
catalyst loading	$\gamma 2 = g_{0new}\ (g_{2new}/g_{2ref})$	$g2 = \text{load}(\%)$
nucleophile	$\gamma 3 = g_{0new}\ (g_{3new}/g_{3ref})$	$g3 = (1 + n(\text{H}))$
solvent	$\gamma 4 = g_{0new}\ (g_{4new}/g_{4ref})$	$g4 = Ds\cdot(Dry + 1)\cdot T\cdot t$
Molecules	**Perturbation terms**	
substrate	ΔVsubs	$V(\text{subs}) = AE$igp of substrate
product	ΔVprod	$V(\text{prod}) = AE$igp of product
catalyst	ΔVcat	$V(\text{cat}) = AE$igp of catalyst
nucleophile	ΔVnuc	$V(\text{nuc}) = AE$igp of nucleophile
solvent	ΔVsolv	$V(\text{solv}) = AE$igp of solvent

[a] DRAGON variables (*V*) $\Delta V_q = V(q)_{nr} - V(q)_{rr}$, with q = substrate (sub), product (prod), … etc.

Table 6. Coefficients and statistical parameters for the PT-QSRR model.

Inputs[a]	B[b]	SE[c]	t[d]	p[e]
a_0	0.558333	0.068850	8.109	<0.05
$g_0 \cdot <ee(\%)>_{nr}$	0.316901	0.001632	194.182	<0.05
$g_{0nr} \cdot g_{4nr}$	−0.000699	0.000002	−333.780	<0.05
$d0 \cdot \Delta V$(subs)	0.132149	0.001197	110.384	<0.05
$d1 \cdot \Delta V$(prod)	−0.001459	0.000615	−2.372	<0.05
$d2 \cdot \Delta V$(cat)	−0.011935	0.000192	−62.049	<0.05
$d3 \cdot \Delta V$(nuc)	−0.136922	0.000759	−180.311	<0.05
$d4 \cdot \Delta V$(solv)	−0.000373	0.000036	−10.328	<0.05

Statistics	Train	Symbol	Validation
N[f]	38419	N	12806
R[g]	0.93	R	0.93
SEE(%)[h]	13.5	SEE(%)	13.5
F[i]	36394	F	84499.01

[a] Input variables of the model. [b] Coefficients of the variables in the model. [c] Standard error (*SE*) of the coefficient. [d] Student *t*-value. [e] *p*-Level of error. [f] Number of cases. [g] Regression coefficient. [h] Standard error of estimates (*SEE*). [i] Fisher ratio.

tions with different substrates, nucleophiles, and catalysts and the scanning of experimental conditions (solvents, temperature, etc.).[57]

To illustrate the practical use of the model in our experimental problem, a series of simulations was performed. Thus, computational screening of the effect of structural changes of the nucleophiles and catalysts on the enantioselectivity of α-amidoalkylation reactions was carried out. First, bicyclic hydroxylactam **1a** was selected as the model substrate under the optimized experimental conditions, that is, THF as the solvent, 40 °C, and 96 h (Table 2).

As the training set (data points used for model development) was limited to a series of enamides, an expanded library of computationally designed enamides and carbamates bearing steric and electronic variations at the nitrogen atom and the aromatic ring was built. It was hypothesized that both positions may contribute synergistically to the selectivity of the system, either by changing the acidity of the NH hydrogen atom and/or the alkene nucleophilicity, which likely modulates the early or late nature of the corresponding transition states involved in the selectivity-determining step (see Figure 2). Regarding the catalyst, a series of chiral Brønsted acids with strong acidic functionalities, such as BINOL-derived phosphoric acids, phosphoramides, and so on, were also computationally designed. In addition, the chiral BINOL framework has been modified, as it has been shown to be crucial in improving the catalyst performance (Figure 3).

Then, this large library of nucleophiles and catalysts was evaluated with the developed PT-QSRR model for the above α-amidoalkylation reaction. A selection of the simulation of the enantioselectivity on a set of 212 catalysts versus 88 nucleophiles is depicted in Figure 4 by using an image with gradient color, which is related to higher (green) or lower (red) *ee*(%), in order to achieve the best visual result.

According to the model, the best results would be expected with *O*-benzyl carbamates **2o–q**, instead of their acetamide

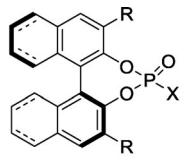

4e-h X = OH **12e-h** X = SH
5e-h X = NHTf **13e-h** [H$_8$] X = $NHSO_2C_4F_9$
10e-h [H$_8$] X = OH **14e-h** [H$_8$] X = $NHSO_2C_8F_{17}$
11e-h [H$_8$] X = NHTf **15e-h** [H$_8$] X = $NHSO_2$-4-CF_3Ph

e R = 3,5-$(CF_3)_2C_6H_3$ **f** R = 4-(2′,4′,6′-$(CH_3)_3C_6H_2)C_6H_4$
g R = 4-(4′-*t*Bu$C_6H_4)C_6H_4$ **h** R = 4-(4′-*t*Bu-2′,6′-$(CH_3)_2C_6H_3)C_6H_4$

Figure 3. Selected catalyst series for the predictions.

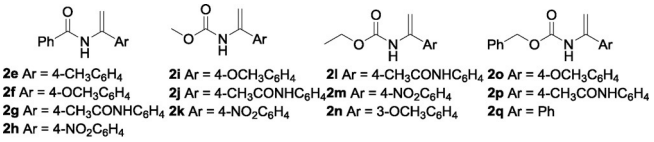

2e Ar = 4-$CH_3C_6H_4$ **2i** Ar = 4-$OCH_3C_6H_4$ **2l** Ar = 4-$CH_3CONHC_6H_4$ **2o** Ar = 4-$OCH_3C_6H_4$
2f Ar = 4-$OCH_3C_6H_4$ **2j** Ar = 4-$CH_3CONHC_6H_4$ **2m** Ar = 4-$NO_2C_6H_4$ **2p** Ar = 4-$CH_3CONHC_6H_4$
2g Ar = 4-$CH_3CONHC_6H_4$ **2k** Ar = 4-$NO_2C_6H_4$ **2n** Ar = 3-$OCH_3C_6H_4$ **2q** Ar = Ph
2h Ar = 4-$NO_2C_6H_4$

	2e	2f	2g	2h	2i	2j	2k	2l	2m	2n	2o	2p	2q
4e	80	85	90	87	80	84	82	88	85	83	98	100	90
4f	79	84	90	86	79	84	81	88	85	83	97	100	90
4g	81	86	91	88	81	85	82	89	86	84	99	100	91
4h	82	87	92	89	82	86	83	90	87	85	100	100	92
5e	82	87	92	89	82	87	84	91	88	85	100	100	92
5f	82	87	92	89	82	86	83	90	87	85	100	100	92
5g	83	88	93	90	83	87	85	91	88	86	100	100	93
5h	84	89	94	91	84	88	86	92	89	87	100	100	94
10e	80	85	90	87	80	85	82	89	86	83	98	100	90
10f	80	85	90	87	80	84	81	88	85	83	98	100	90
10g	81	86	91	88	81	85	83	89	86	84	99	100	91
10h	82	87	92	89	82	86	84	90	87	85	100	100	92
11e	82	87	93	89	82	87	84	91	88	85	100	100	93
11f	82	87	92	89	82	86	84	90	87	85	100	100	92
11g	83	88	93	90	83	88	85	91	89	86	100	100	93
11h	84	89	94	91	84	89	86	92	90	87	100	100	94
12e	80	85	90	87	80	84	82	88	85	83	98	100	90
12f	79	84	90	86	79	84	81	88	85	83	97	100	90
12g	81	86	91	88	81	85	82	89	86	84	99	100	91
12h	81	87	92	89	82	86	83	90	87	85	100	100	92
13e	86	91	96	93	86	90	88	94	91	89	100	100	96
13f	86	91	96	93	86	90	87	94	91	89	100	100	96
13g	87	92	97	94	87	91	89	95	92	90	100	100	97
13h	88	93	98	95	88	92	90	96	93	91	100	100	98
14e	92	97	100	99	92	96	93	100	97	95	100	100	100
14f	91	96	100	98	92	96	93	100	97	95	100	100	100
14g	93	98	100	100	93	97	95	100	98	96	100	100	100
14h	94	99	100	100	94	98	96	100	100	97	100	100	100
15e	84	89	95	91	84	89	86	93	90	87	100	100	95
15f	84	89	94	91	84	88	86	92	89	87	100	100	94
15g	85	90	95	92	85	90	87	94	91	88	100	100	95
15h	86	91	96	93	86	91	88	95	92	89	100	100	96

Figure 4. Selected *ee*(%) predicted for intermolecular α-amidoalkylation reaction.[58]

counterparts, under the above indicated experimental conditions, with almost all catalysts tested.

Besides, the predictions indicated that high enantioselectivities would be obtained if these types of carbamates had an electron-donor substituent (OCH_3, $NHCOCH_3$) in the *para* position, whereas the presence of a chlorine atom would lead to a decrease in the predicted *ee*(%), in agreement with our experimental results. Interestingly, the screening revealed that the best *ee*(%) would be obtained by employing chiral Brønsted acids **13**–**15** and incorporating a sterically demanding H8-binaphthyl moiety instead of the unsaturated analogues, in particular, phosphoramides $(RO)_2PONHSO_2C_8H_{17}$ **14e–h** with the bulkiest aromatic substituents in the BINOL framework (Figure 4).

On the other hand, the use of atom stochastic moments enables back-projection of the model onto the enantioselectivity,[59] that is, a map projecting the contribution of each atom or group of atoms to the enantioselectivity can be drawn. The back-projection map of the catalytic activity of the biphenyl-substituted phosphoramide **14h** is depicted in Table 7, showing how the different electronic and steric variations on the catalyst affect the predicted *ee*(%) values. Thus, the presence of the substituted biphenyl system on the BINOL framework is crucial to obtain high levels of enantioselectivity. If either of these aryl groups is removed, the predicted enantioselectivity would decrease. Therefore, there is an excellent match between the prediction and experimental results.

Table 7. Back-projection map analysis of the catalytic activity of the biphenyl substituted phosphoramide **14h**.

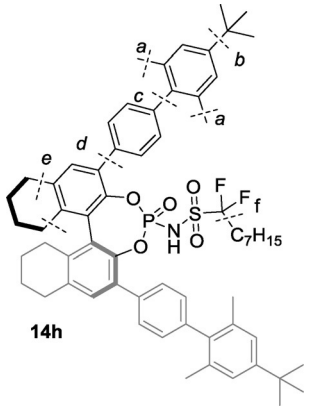

14h

ee[%]$_{ref}$	ee[%]$_{new}$	ΔV (ee[%]$_{ref}$−ee[%]$_{new}$)
83.8	a 82.6	1.7
	b 80.4	3.4
	c 75.1	8.7
	d 72.2	11.6
	e 82.0	1.8
	f 73.8	10.0

Another important application of the developed model lies with its potential to predict the enantioselectivity outcomes of new hydroxylactam substrates. To define the substrate scope, acetamide **2a** was selected as the nucleophile and a similar study of substrates versus catalysts was carried out. As in the previous case, we first selected a series of well-known substrates and catalysts from the literature. Then, the library was expanded with the computationally designed chiral Brønsted acids and a series of hydroxylactams (cyclic and bicyclic cores with different substitution patterns). Next, the *ee*(%) values were predicted with the model for the standard α-amidoalkylation reaction conditions (THF as the solvent, 40 °C, 96 h) of these new hydroxylactams. As an example, Table 8 shows the back-projection map analysis of the enantioselectivity for substrates **1a** and **1c.** The model predicts that benzo-fused hydroxylactams would lead to lower *ee*(%) values in the α-amidoalkylation reactions. Besides, the substituents on the aromatic ring of the isoquinoline moiety seem to play an important role.

Table 8. Back-projection map analysis of the enantioselectivity of substrates **1a** and **1c**.

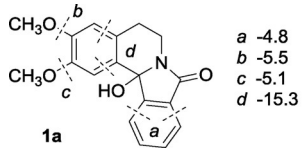

1a **1c**

ee[%]$_{ref}$ **1a/c**	ee[%]$_{new}$ **1a/c**	ΔV (ee[%]$_{ref}$−ee[%]$_{new}$) **1a/c**
68.2/89.0	a 73/90.1	a 4.8/1.1
	b 73.7/91.0	b 5.5/2
	c 73.3	c 5.1
	d 83.5	d 15.3

In view of these results, we decided to study the effect of physicochemical parameters of substituents in different positions (*ortho*, *para*, and *meta*) of the benzene rings, both on the isoquinoline and isoindole moieties, on the enantioselectivity. For this purpose, one of the reactions that provided a higher *ee*(%) in our experimental study (Table 2, entry 1) was selected as the reaction of reference. Then, different derivatives of the substrate introducing both electron-donating and electron-withdrawing substituents in those positions were computationally created. Next, the eigenvalues of these derivatives were calculated and introduced into Equation (1) to predict the new *ee*(%) values. Finally, a simple linear regression analysis of the *ee*(%) versus different constants of the substituents was carried out. Specifically, the Hammett parameters (σ_p^+ and σ_p) to measure electronic effects with and without the creation of electrostatic charge in the center of reaction[60] were selected. In addition, the Charton constants (υ)[61] to measure steric effects on *ortho* positions were used. The Hammet constants did not show significant correlations with the *ee*(%) values (see the Supporting Information). In contrast, the υ values showed a significant negative correlation $R^2 = 0.89$ $p < 0.05$ with *ee*(%) in different positions of both rings, as shown in Figure 5, which indicates that the steric hindrance of the substituents of the sub-

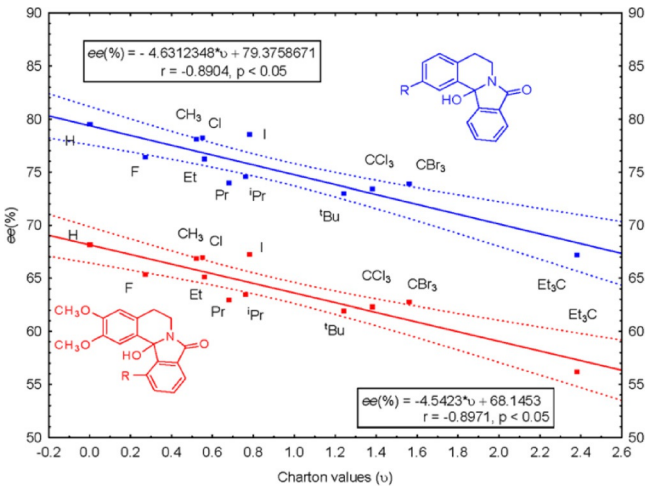

Figure 5. Predicted *ee*(%) versus Charton parameter values.

strate would hinder the arrangement of the substrate in the chiral pocket of the catalyst. These predictions are in agreement with the proposed model (see Figure 2).[62]

3. Conclusions

Enantioselective α-amidoalkylation reaction of enamides with bicyclic α-hydroxylactams catalyzed by chiral BINOL-derived phosphoric acids allows the introduction of new functionality (an acylmethyl group) in the new generated quaternary stereocenter at the C-1 position of the tetrahydroisoquinoline unit of the isoindoloisoquinoline skeleton. To achieve reasonable levels of enantioselectivity, either the enamides used as nucleophiles or the substrates should have a free N–H group, which would indicate that hydrogen-bonding interactions of the phosphate ion-paired intermediate to the N–H bonds could potentially be involved. As the understanding of how the different parameters affect the stereochemical outcomes of these reactions is still difficult to rationalize, a correlative PT-QSRR model has been developed to find trends that improve the experiment without engaging in a long-term empirical investigation. The QSRR model predicts the effect of the substituents on the aromatic rings of the enamides or hydroxylactams, as well as the substitution pattern of the catalysts. For example, a relationship between steric parameters (Charton parameters) of substrate substituents and enantiomeric ratios of the products could be established. Besides, the best *ee* would be expected with *O*-benzyl carbamates with an electron-donor substituent (OCH_3, $NHCOCH_3$) in the *para* position, with chiral phosphoramides incorporating a sterically demanding H8-binaphthyl moiety, in particular, $(RO)_2PONHSO_2C_8H_{17}$ **14e–h** with the bulkiest aromatic substituents in the BINOL framework. Therefore, the developed model is expected to be useful as a reference tool to choose the adequate catalyst or experimental conditions for enantioselective α-amidoalkylation reactions.

Experimental Section

Model Development

The PT-QSRR model is a QSRR based on PT ideas. Consequently, the model begins with the expected value $ee(\%)_{expected} = <ee(\%)>_{new}$ and the perturbation terms are added. We have two types of perturbation terms. One type is the intensity factors g_q that accounts only for non-structural intensity factors f_q (temperature, time, solvent dipole, etc.) in the new reaction. We calculated the g_q as products of all factors considered to affect the molecules of class q^{th}. The second type of perturbation factor is the $\gamma_q \cdot \Delta V(m_q)$ terms. These perturbation terms accounts for changes in both intensity factors and chemical structure. Consequently, they are the product of the switching functions $\gamma_q = g_{0new} \cdot (g_{qnew}/g_{qref})$ used to quantify the changes on intensity factors and shifting functions $\Delta V(m_q) = V(m_q)_{new} - V(m_q)_{ref}$ for structural changes on different classes of molecules. The five classes of molecules are, according to their different roles in the reaction, m_0 = substrate (sub), m_1 = product (prod), m_2 = catalyst (cat), m_3 = nucleophile (nuc), and m_4 = solvent (solv). This second set of functions involves molecular descriptors of chemical structures calculated with the software DRAGON.[55] The molecular descriptors used in this study were the absolute eigenvalues of the matrix of topological distance weighted with atomic polarizabilities $V(mq) = AE_{igpq}$. The final formula of the model considered an initial term $ee(\%)_{expected}$, additive terms for the conditions of the new reaction, and multiplicative terms for the intensity factors and structural changes. The formula of the model used is given in Equation (2):

$$ee(\%)_{new} = a_0 + a_1 \cdot g_{0new} \cdot \langle ee(\%)_{new} \rangle + \sum_{q=2}^{q=6} a_q \cdot g_{0new} \cdot g_{qnew} \sum_{q=1}^{q=6} a_q \cdot \gamma_q \cdot \Delta V(m_q) \quad (2)$$

General Procedure for the Synthesis of Enantioenriched Isoindolo[1,2-*a*]isoquinolines 3aa–ac and 3ba–bb from Enamides 2a–c

A solution of 12b-hidroxyisoindoloisoquinolone **1a** (0.2 mmol), enamides **2a–c** (0.4 mmol) and catalyst **4d** in dry THF (5 mL) was stirred during 96 h at 40 °C. The reaction was quenched by addition of HCl (1 M, 1 mL) and then satuarated $NaHCO_3$ (1 mL). The aqueous phase was extracted with CH_2Cl_2 (3×10 mL). The combined organic extracts were dried over Na_2SO_4 and concentrated. The crude reaction mixture was purified by column chromatography (alumina) to afford the corresponding enantioenriched isoindolo[1,2-*a*]isoquinolones **3aa–ac**.

Acknowledgements

Ministerio de Economía y Competitividad (CTQ2013-41229-P), IKERBASQUE foundation, Gobierno Vasco (IT-623-13) and Universidad del País Vasco/Euskal Herriko Unibertsitatea UPV/EHU are gratefully acknowledged for their financial support. Technical and human support provided by Servicios Generales de Investigación SGIker (UPV/EHU, MINECO, GV/EJ, ERDF and ESF) is also acknowledged.

Keywords: amidoalkylation · asymmetric catalysis · cheminformatics · chiral Brønsted acids · quantitative structure–reactivity relationships

[1] For general reviews on *N*-acyliminium ions, see: a) W. N. Speckamp, H. Hiemstra, *Tetrahedron* **1985**, *41*, 4367–4416; b) W. N. Speckamp, M. J. Moolenaar, *Tetrahedron* **2000**, *56*, 3817–3856; c) A. Yazici, S. G. Pyne, *Synthesis* **2009**, 339–368; d) A. Yazici, S. G. Pyne, *Synthesis* **2009**, 513–541; e) S. T. Le Quement, R. Petersen, M. Meldal, T. E. Nielsen, *Biopolymers* **2010**, *94*, 242–256; f) U. Martínez-Estibalez, A. Gómez-SanJuan, O. García-Calvo, E. Aranzamendi, E. Lete, N. Sotomayor, *Eur. J. Org. Chem.* **2011**, 3610–3633.

[2] For representative examples from our group, see: a) I. Osante, M. I. Collado, E. Lete, N. Sotomayor, *Eur. J. Org. Chem.* **2001**, 1267–1277; b) I. González-Temprano, N. Sotomayor, E. Lete, *Synlett* **2002**, 0593–0597; c) I. González-Temprano, I. Osante, E. Lete, N. Sotomayor, *J. Org. Chem.* **2004**, *69*, 3875–3885; d) M. N. Abdullah, S. Arrasate, E. Lete, N. Sotomayor, *Tetrahedron* **2008**, *64*, 1323–332.

[3] For a review, see: a) R. Mazurkiewicz, A. Pazdzierniok-Holewa, J. Adamek, K. Zielinska, *Adv. Heterocycl. Chem.* **2014**, *111*, 43–94. For selected examples, see: b) I. Osante, E. Lete, N. Sotomayor, *Tetrahedron Lett.* **2004**, *45*, 1253–1256; c) F. Pin, S. Comesse, B. Garrigues, S. Marchalin, A. Daiech, *J. Org. Chem.* **2007**, *72*, 1181–1191; d) L. Boiaryna, M. K. El Mkaddem, C. Taillier, V. Dalla, M. Othman, *Chem. Eur. J.* **2012**, *18*,

14192 – 14200; e) A. K. Maity, S. Roy, *Adv. Synth. Catal.* **2014**, *356*, 2627 – 2642.

[4] See for example: a) T. E. Nielsen, M. Meldal, *Curr. Opin. Drug Discov. Develop.* **2009**, *12*, 798 – 810; b) C. Avendaño, E. de la Cuesta in *Advances in Organic Synthesis Vol. 5* (Ed.: A. U. Rahman), Bentham Science, Hilversum, **2013**, pp. 309—354.

[5] Y.-S. Lee, M. Alam, R. S. Keri, *Chem. Asian J.* **2013**, *8*, 2906 – 2919.

[6] For reviews on asymmetric organocatalytic Friedel–Crafts reactions, see: a) *Catalytic Asymmetric Friedel – Crafts Alkylations* (Eds.: M. Bandini, A. Umani-Ronchi), Wiley-VCH, Weinheim, **2009**; b) S.-L. You, Q. Cai, M. Zeng, *Chem. Soc. Rev.* **2009**, *38*, 2190 – 2201; c) V. Terrasson, R. M. de Figueiredo, J. M. Campagne, *Eur. J. Org. Chem.* **2010**, 2635 – 2655; d) M. Zeng, S.-L. You, *Synlett* **2010**, 1289 – 1301; e) R. M. de Figueiredo, J. M. Campagne in *Comprehensive Enantioselective Organocatalysis, Vol. 3* (Ed.: P. I. Dalko), Wiley-VCH, Weiheim, **2013**, pp. 1043 – 1066; f) I. P. Beletskaya, A. D. Averin, *Curr. Organocatal.* **2016**, *3*, 60 – 83.

[7] For selected recent reviews, see: a) Y. Takemoto, *Chem. Pharm. Bull.* **2010**, *58*, 593 – 601; b) W.-Y. Siau, J. Wang, *Catal. Sci. Technol.* **2011**, *1*, 1298 – 1310; c) E. Marqués-López, R. P. Herrera in *New Strategies in Chemical Synthesis and Catalysis* (Ed.: B. Pignataro), Wiley-VCH, Weiheim, **2012**, pp. 175 – 199; d) G. Jakab, P. R. Schreiner in *Comprehensive Enantioselective Organocatalysis, Vol. 2* (Ed.: P. I. Dalko), Wiley-VCH, Weiheim, **2013**, pp. 315 – 341; e) S. Narayanaperumal, D. G. Rivera, R. C. Silva, M. W. Paixao, *ChemCatChem* **2013**, *5*, 2756 – 2773; f) O. V. Serdyuk, C. M. Heckel, S. B. Tsogoeva, *Org. Biomol. Chem.* **2013**, *11*, 7051 – 7071; For seminal studies, see: g) M. S. Sigman, E. N. Jacobsen, *J. Am. Chem. Soc.* **1998**, *120*, 4901 – 4902; h) T. Okino, Y. Hoashi, Y. Takemoto, *J. Am. Chem. Soc.* **2003**, *125*, 12672 – 12673.

[8] For selected recent reviews, see: a) D. Kampen, C. M. Reisinger, B. List, *Top. Curr. Chem.* **2010**, *291*, 395 – 456; b) M. Terada, *Synthesis* **2010**, 1929 – 1982; c) A. Zamfir, S. Schenker, M. Freund, S. B. Tsogoeva, *Org. Biomol. Chem.* **2010**, *8*, 5262 – 5276; d) M. Terada, *Curr. Org. Chem.* **2011**, *15*, 2227 – 2256; e) T. Akiyama in *Asymmetric Synthesis II* (Eds.: M. Christmann, S. Brase), Wiley-VCH, Weinheim, **2012**, pp. 261 – 266; f) K. Mori, T. Akiyama in *Comprehensive Enantioselective Organocatalysis, Vol. 2* (Ed.: P. I. Dalko), Wiley-VCH, Weiheim, **2013**, pp. 289 – 314; g) M. Terada, N. Momiyama in *Science of Synthesis Asymmetric Organocatalysis, Vol. 2* (Eds.: B. List, K. Maruoka), Thieme, Stuttgart, **2012**, pp. 219 – 278; h) J. Lv, S. Luo, *Chem. Commun.* **2013**, *49*, 847 – 858; i) R. Zhao, L. Shi, *ChemCatChem* **2014**, *6*, 3309 – 3311; j) D. Parmar, E. Sugiono, S. Raja, M. Rueping, *Chem. Rev.* **2014**, *114*, 9047 – 915; For seminal studies, see: k) T. Akiyama, J. Itoh, K. Yokota, K. Fuchibe, *Angew. Chem. Int. Ed.* **2004**, *43*, 1566 – 1568; *Angew. Chem.* **2004**, *116*, 1592 – 1594; l) D. Uraguchi, M. Terada, *J. Am. Chem. Soc.* **2004**, *126*, 5356 – 5357.

[9] a) S. J. Connon, *Angew. Chem. Int. Ed.* **2006**, *45*, 3909 – 3912; *Angew. Chem.* **2006**, *118*, 4013 – 4016; b) T. Akiyama in *Science of Synthesis Asymmetric Organocatalysis, Vol. 2* (Eds.: B. List, K. Maruoka), Thieme, Stuttgart, **2012**, pp. 169 – 217; c) M. Terada, N. Momiyama in *Science of Synthesis Asymmetric Organocatalysis, Vol. 2* (Eds.: B. List, K. Maruoka), Thieme, Stuttgart, **2012**, pp. 219 – 278.

[10] a) M. Zeng, S.-L. You, *Synlett* **2010**, 1289 – 1301; b) H. Wu, Y.-P. He, F. Shi, *Synthesis* **2015**, *47*, 1990 – 2016; c) R. Dalpozzo, *Chem. Soc. Rev.* **2015**, *44*, 742 – 778.

[11] For selected asymmetric organocatalytic Friedel–Crafts reactions of ketimines, see: a) Y. X. Jia, J. Zhong, S. F. Zhu, C. M. Zhang, Q. L. Zhou, *Angew. Chem. Int. Ed.* **2007**, *46*, 5565 – 5567; *Angew. Chem.* **2007**, *119*, 5661 – 5663; b) R. Husmann, E. Sugiono, S. Mersmann, G. Raabe, M. Rueping, C. Bolm, *Org. Lett.* **2011**, *13*, 1044 – 1047; c) M. Rueping, S. Raja, A. Nuñez, *Adv. Synth. Catal.* **2011**, *353*, 563 – 568; d) Q. Yin, S. L. You, *Chem. Sci.* **2011**, *2*, 1344 – 1348; e) Y. Qian, C. Jing, C. Zhai, W. Hu, *Adv. Synth. Catal.* **2012**, *354*, 301 – 307; f) A. Gómez-SanJuan, N. Sotomayor, E. Lete *Tetrahedron Lett.* **2012**, *53*, 2157 – 2159;g) J. C. Feng, W. J. Yan, D. Wang, P. Li, Q. T. Sun, R. Wang, *Chem. Commun.* **2012**, *48*, 8003 – 8005; h) K. F. Zhang, J. Nie, R. Guo, Y. Zheng, J. A. Ma, *Adv. Synth. Catal.* **2013**, *355*, 3497 – 3502; i) T. Kano, R. Takechi, R. Kobayashi, K. Maruoka, *Org. Biomol. Chem.* **2014**, *12*, 724 – 727.

[12] E. Aranzamendi, N. Sotomayor, E. Lete, *J. Org. Chem.* **2012**, *77*, 2986 – 2991.

[13] See, for example: a) P. Li, H. Yamamoto, *Top. Organomet. Chem.* **2011**, *37*, 161 – 183; b) P. Chauhan, S. S. Chimni, *RSC Adv.* **2012**, *2*, 737 – 758.

[14] F. Fang, G. Hua, F. Shi, P. Li, *Org. Biomol. Chem.* **2015**, *13*, 4395 – 4398.

[15] Q. Yin, S.-G. Wang, S.-L. You, *Org. Lett.* **2013**, *15*, 2688 – 2691.

[16] H.-H. Zhang, Y.-M. Wang, Y.-W. Xie, Z.-Q. Zhu, F. Shi, S.-J. Tu, *J. Org. Chem.* **2014**, *79*, 7141 – 7151.

[17] a) D. Zhou, Z. Huang, X. Yu, Y. Wang, J. Li, W. Wang, H. Xie, *Org. Lett.* **2015**, *17*, 5554 – 5557. See also: b) M. Montesinos-Magraner, C. Vila, R. Canton, G. Blay, I. Fernández, M. C. Muñoz, J. R. Pedro, *Angew. Chem. Int. Ed.* **2015**, *54*, 6320 – 6324; *Angew. Chem.* **2015**, *127*, 6418 – 6422.

[18] Q.-X. Guo, Y.-G. Peng, J.-W. Zhang, L. Song, Z. Feng, L.-Z. Gong, *Org. Lett.* **2009**, *11*, 4620 – 4623.

[19] C. Guo, J. Song, J.-Z. Huang, P.-H. Chen, S.-W. Luo, L.-Z. Gong, *Angew. Chem. Int. Ed.* **2012**, *51*, 1046 – 1050; *Angew. Chem.* **2012**, *124*, 1070 – 1074.

[20] For selected reviews; see: a) J. D. Scott, JR. M. Williams, *Chem. Rev.* **2002**, *102*, 1669 – 173; b) K. W. Bentley, *Nat. Prod. Rep.* **2006**, *23*, 444 – 463; and previous reports in this series; c) U. Pässler, H. J. Knöller in *The Alkaloids: Chemistry and Biology, Vol. 70* (Ed.: H. J. Knöller), Elsevier, Amsterdam, **2011**, pp. 79 – 151; d) L. Antkiewicz-Michaluk, H. Rommelspacher, Eds. *Isoquinolines and Beta-Carbolines as Neurotoxins and Neuroprotectants: New Vistas In Parkinson's Disease Therapy, Current Topics In Neurotoxicity*, Springer, New York, **2012**.

[21] J. Semenas, A. Hedblom, R. R. Miftakhova, M. Sarwar, R. Larsson, L. Shcherbina, M. E. Johansson, P. Haerkoenen, O. Sterner, J. L. Persson, *Proc. Natl. Acad. Sci. USA* **2014**, *111*, E3689 – E3698.

[22] a) K. Speck, T. Magauer, *Beilstein J. Org. Chem.* **2013**, *9*, 2048 – 2078; b) P. Kittakoop, C. Mahidol, S. Ruchirawat, *Curr. Top. Med. Chem.* **2014**, *14*, 239 – 252.

[23] a) T. R. Belliotti, W. A. Brink, S. R. Kesten, J. R. Rubin, D. J. Wustrow, K. T. Zoski, S. Z. Whetzel, A. E. Corbin, T. A. Pugsley, T. G. Heffner, L. D. Wise, *Bioorg. Med. Chem. Lett.* **1998**, *8*, 1499 – 1502; b) J. N. Oak, J. Oldenhof, H. H. Van Tol, *Eur. J. Pharmacol.* **2000**, *405*, 303 – 327; c) L. A. Sorbera, P. A. Leeson, J. Silvestre, J. Castaner, *Drugs Future* **2001**, *26*, 651 – 657; d) J. R. Atack, *Expert Opin. Invest. Drugs* **2005**, *14*, 601 – 618; e) L. Richter, C. de Graaf, W. Sieghart, Z. Varagic, M. Moerzinger, I. J. P. de Esch, G. F. Ecker, M. Ernst, *Nat. Chem. Biol.* **2012**, *8*, 455 – 464.

[24] For the synthesis of tetrahydroisoquinolines, see: a) M. Chrzanowska, M. D. Rozwadowska, *Chem. Rev.* **2004**, *104*, 3341 – 3370; b) K. Pulka, *Curr. Opin. Drug Discov. Devel.* **2010**, *13*, 669 – 684; c) J. Stöckigt, A. P. Antonchick, F. Wu, H. Waldmann, *Angew. Chem. Int. Ed.* **2011**, *50*, 8538 – 8564; *Angew. Chem.* **2011**, *123*, 8692 – 8719; d) K. Koketsu, A. Minami, K. Watanabe, H. Oguri, H. Oikawa, *Curr. Opin. Chem. Biol.* **2012**, *16*, 142 – 149. For the synthesis of isoindoles, see: e) G. Stajer, F. Csende, *Curr. Org. Chem.* **2005**, *9*, 1277 – 1286; f) A. di Mola, L. Palombi, A. Massa in *Targets in Heterocyclic Systems, Vol. 18* (Eds.: O. A. Attanasi, R. Noto, D. Spinelli), Società Chimica Italiana, Roma, **2014**, pp. 113 – 140; g) B. Ye, N. Cramer, *Acc. Chem. Res.* **2015**, *48*, 1308 – 1318; h) H. S. P. Rao, A. V. B. Rao, *J. Org. Chem.* **2015**, *80*, 1506 – 1516, and references therein.

[25] For selected synthetic approaches to these alkaloids, see: a) A. Padwa, M. D. Danca, K. I. Hardcastle, M. S. McLure, *J. Org. Chem.* **2003**, *68*, 929 – 941; b) A. Moreau, A. Couture, E. Deniau, P. Grandclaudon, S. Lebrun, *Eur. J. Org. Chem.* **2005**, 3437 – 3442; c) J.-Y. Min, G. Kim, *J. Org. Chem.* **2014**, *79*, 1444 – 1448; d) J. Selvakumar, R. S. Rao, V. Srinivasapriyan, S. Marutheeswaran, C. R. Ramanathan, *Eur. J. Org. Chem.* **2015**, 2175 – 2188.

[26] A. Suyavaran, C. Ramamurthy, R. Mareeswaran, Y. V. Shanthi, J. Selvakumar, S. Mangalaraj, M. S. Kumar, C. R. Ramanathan, C. Thirunavukkarasu, *Bioorg. Med. Chem.* **2015**, *23*, 488 – 498.

[27] T. Akiyama, K. Mori, *Chem. Rev.* **2015**, *115*, 9277 – 9306, and references therein.

[28] G. B. Rowland, H. L. Zhang, E. B. Rowland, S. Chennamadhavuni, Y. Wang, J. C. Antilla, *J. Am. Chem. Soc.* **2005**, *127*, 15696 – 15697.

[29] a) P. García-García, F. Lay, P. García-García, C. Rabalakos, B. List, *Angew. Chem. Int. Ed.* **2009**, *48*, 4363 – 4366; *Angew. Chem.* **2009**, *121*, 4427 – 4430; b) A. Galván, A. B. González-Pérez, R. Álvarez, A. R. De Lera, F. J. Fañanás, F. Rodríguez, *Angew. Chem. Int. Ed.* **2016**, *55*, 3428 – 3432; *Angew. Chem.* **2016**, *128*, 3489 – 3493.

[30] T. Akiyama, Y. Saitoh, H. Morita, K. Fuchibe, *Adv. Synth. Catal.* **2005**, *347*, 1523 – 1526.

[31] C. Baudequin, A. Zamfir, S. B. Tsogoeva, *Chem. Commun.* **2008**, 4637 – 4639.

[32] H. Kim, E. Sugiono, Y. Nagata, M. Wagner, M. Bonn, M. Rueping, J. Hunger, *ACS Catal.* **2015**, *5*, 6630 – 6633.

[33] See Supporting Information for the preparation of enamides **2a–d**.
[34] CCDC 1504521 contains the supplementary crystallographic data for this paper. These data can be obtained free of charge from The Cambridge Crystallographic Data Centre.
[35] Reviews for counteranion directed catalysis: a) S. Schenker, A. Zamfir, M. Freund, S. B. Tsogoeva, *Eur. J. Org. Chem.* **2011**, 2209 – 2222; b) M. Rueping, B. J. Nachtsheim, W. Ieawsuwan, I. Atodiresei, *Angew. Chem. Int. Ed.* **2011**, *50*, 6706 – 6720; *Angew. Chem.* **2011**, *123*, 6838 – 6853; c) M. Mahlau, B. List, *Angew. Chem. Int. Ed.* **2013**, *52*, 518 – 533; *Angew. Chem.* **2013**, *125*, 540 – 556; d) R. J. Phipps, G. L. Hamilton, F. D. Toste, *Nat. Chem.* **2012**, *4*, 603 – 6014.
[36] L. Simón, J. M. Goodman, *J. Org. Chem.* **2011**, *76*, 1775 – 1788.
[37] This type of dual activation has been previously established by DFT calculations, see Ref. [19].
[38] The configuration of **3ba** has been assigned assuming a uniform mechanism.
[39] a) L. Simón, J. M. Goodman, *J. Am. Chem. Soc.* **2008**, *130*, 8741 – 8747; b) T. Marcelli, P. Hammar, F. Himo, *Chem. Eur. J.* **2008**, *14*, 8562 – 8571; c) L. Simón, J. M. Goodman, *J. Org. Chem.* **2010**, *75*, 589 – 597; d) Y. Shibata, M. Yamanaka, *J. Org. Chem.* **2013**, *78*, 3731 – 3736; e) K. Saito, Y. Shibata, M. Yamanaka, T. Akiyama, *J. Am. Chem. Soc.* **2013**, *135*, 11740 – 11743; f) K. Saito, K. Horiguchi, Y. Shibata, M. Yamanaka, T. Akiyama, *Chem. Eur. J.* **2014**, *20*, 7616 – 7620.
[40] a) A. Kondoh, Y. Ota, T. Komuro, F. Egawa, K. Kanomata, M. Terada, *Chem. Sci.* **2016**, *7*, 1057 – 1062. For a related study of the reaction of vinyl indoles and azalactones catalyzed by chiral phosphoric acids, see: b) K. Kanomata, M. Terada, *Synlett* **2016**, *27*, 581 – 585.
[41] a) H. Satoh, O. Sacher, T. Nakata, L. Chem, J. Gasteiger, K. Funatsu, *J. Chem. Inf. Comput. Sci.* **1998**, *38*, 210 – 219; b) S. Patel, J. Rabone, S. Russel, J. Tissen, W. Klaffke, *J. Chem. Inf. Comput. Sci.* **2001**, *41*, 926 – 933.
[42] a) K. C. Harper, E. N. Bess, M. S. Sigman, *Nat. Chem.* **2012**, *4*, 366 – 374; b) K. C. Harper, M. S. Sigman, *J. Org. Chem.* **2013**, *78*, 2813 – 2818; c) E. N. Bess, A. J. Bischoff, M. S. Sigman, *Proc. Natl. Acad. Sci. USA* **2014**, *111*, 14698 – 14703 and references therein.
[43] K. C. Harper, M. S. Sigman, *Proc. Natl. Acad. Sci. USA* **2011**, *108*, 2179 – 2183.
[44] a) K. C. Harper, S. C. Vilardi, M. S. Sigman, *Science* **2011**, *333*, 1875 – 18787; b) K. C. Harper, S. C. Vilardi, M. S. Sigman, *J. Am. Chem. Soc.* **2013**, *135*, 2482 – 2485.
[45] a) C. Zhang, C. B. Santiago, J. M. Crawford, M. S. Sigman, *J. Am. Chem. Soc.* **2015**, *137*, 15668 – 15671; b) C. Zhang, C. B. Santiago, L. Kou, M. S. Sigman, *J. Am. Chem. Soc.* **2015**, *137*, 7290 – 7293.
[46] S. Aguado-Ullate, M. Urbano-Cuadrado, I. Villalba, E. Pires, J. I. García, C. Bo, J. J. Carbó, *Chem. Eur. J.* **2012**, *18*, 14026 – 14036.
[47] H. Huang, H. Zong, G. Bian, H. Yue, L. Song, *J. Org. Chem.* **2014**, *79*, 9455 – 9464.
[48] A. Milo, A. J. Neel, F. D. Toste, M. S. Sigman, *Science* **2015**, *347*, 737 – 743.
[49] H. González-Díaz, S. Arrasate, A. Gómez-SanJuan, N. Sotomayor, E. Lete, L. Besada-Porto, J. M. Ruso, *Curr. Top. Med. Chem.* **2013**, *13*, 1713 – 1741.
[50] F. Luan, VV. Kleandrova, H. González-Díaz, J. M. Ruso, A. Melo, A. Speck-Planche, M. N. Cordeiro, *Nanoscale* **2014**, *6*, 10623 – 10630.
[51] C. R. Munteanu, J. Dorado, A. Pazos Sierra, F. Prado-Prado, L. G. Pérez-Montoto, S. Vilar, F. M. Ubeira, A. Sánchez-González, M. Cruz-Monteagudo, S. Arrasate, N. Sotomayor, E. Lete, A. Duardo-Sánchez, A. Díaz-López, G. Patlewicz, H. González-Díaz in *Towards an Information Theory of Complex Networks. Statistical Methods and Applications* (Eds.: M. Dehmer, F. Emmert-Streib, A. Mehler), Springer, Basel, **2011**, pp. 199 – 258.
[52] C. Blázquez-Barbadillo, E. Aranzamendi, E. Coya, E. Lete, N. Sotomayor, H. González-Díaz, *RSC Adv.* **2016**, *6*, 38602 – 38610.
[53] H. Gonzalez-Diaz, S. Arrasate, A. Gómez-SanJuan, N. Sotomayor, E. Lete, A. Speck-Planche, J. M. Ruso, F. Luan, M. N. Cordeiro, *Curr. Drug Metab.* **2014**, *15*, 470 – 488.
[54] a) Y. Xie, Y. Zhao, B. Qian, L. Yang, C. Xia, H. Huang, *Angew. Chem. Int. Ed.* **2011**, *50*, 5682 – 5686; *Angew. Chem.* **2011**, *123*, 5800 – 5804; b) X. Yu, A. Lu, Y. Wang, G. Wu, H. Song, Z. Zhou, C. Tang, *Eur. J. Org. Chem.* **2011**, 892 – 897; c) X. Yu, A. Lu, Y. Wang, G. Wu, H. Song, Z. Zhou, C. Tang, *Eur. J. Org. Chem.* **2011**, 3060 – 3066; d) T. Courant, S. Kumarn, L. He, P. Retailleau, G. Masson, *Adv. Synth. Catal.* **2013**, *355*, 836 – 840.
[55] a) E. Papa, F. Villa, P. Gramatica, *J. Chem. Inf. Model.* **2005**, *45*, 1256 – 1266; b) A. Mauri, V. Consonni, M. Pavan, R. Todeschini, *MATCH* **2006**, *56*, 237 – 248; c) M. Helguera, R. D. Combes, M. Pérez González, M. N. D. S. Cordeiro, *Curr. Top. Med. Chem.* **2008**, *8*, 1628 – 1655. The structure of the molecules was uploaded to the software DRAGON as SMILE codes: d) M. A. Siani, D. Weininger, J. M. Blaney, *J. Chem. Inf. Comput. Sci.* **1994**, *34*, 588 – 593; e) M. A. Siani, D. Weininger, C. A. James, J. M. Blaney, *J. Chem. Inf. Comput. Sci.* **1995**, *35*, 1026 – 1033; f) A. Karwath, L. De Raedt, *J. Chem. Inf. Model.* **2006**, *46*, 2432 – 2444; g) A. A. Toropov, E. Benfenati, *Curr. Drug Discovery Technol.* **2007**, *4*, 77 – 116; h) A. A. Toropov, A. P. Toropova, E. Benfenati, D. Leszczynska, J. Leszczynski, *J. Comput. Chem.* **2010**, *31*, 381 – 392.
[56] T. Hill, P. Lewicki, *Statistics, Methods and Applications*, Stat Soft Inc., Tulsa, **2006**.
[57] As an example, predicted *ee*(%) for a model reaction when changing temperature *vs* solvent are shown in the Supporting information.
[58] See Supporting information for the structures and numbering of all catalysts and nucleophiles.
[59] a) O. Gia, S. Marciani Magno, E. Quesada, L. Santana, E. Uriarte, L. Dalla Via, *Bioorg. Med. Chem.* **2005**, *13*, 809 – 817; b) H. González-Díaz, E. Olazábal, L. Santana, E. Uriarte, Y. González-Díaz, N. Castañedo, *Bioorg. Med. Chem.* **2007**, *15*, 962 – 968.
[60] a) L. Hammett, *Chem. Rev.* **1935**, *17*, 125 – 136; b) L. P. Hammett, *J. Am. Chem. Soc.* **1937**, *59*, 96 – 103.
[61] a) M. Charton, *J. Am. Chem. Soc.* **1975**, *97*, 1552 – 1556; b) M. Charton, *J. Am. Chem. Soc.* **1975**, *97*, 3691 – 3693; c) M. Charton, *J. Am. Chem. Soc.* **1975**, *97*, 3694 – 3697; d) M. Charton, *J. Org. Chem.* **1976**, *41*, 2217 – 2220.
[62] See Supporting Information for additional graphical representation of predicted *ee* (%) vs. Charton parameter.

Received: September 30, 2016
Published online on November 23, 2016

